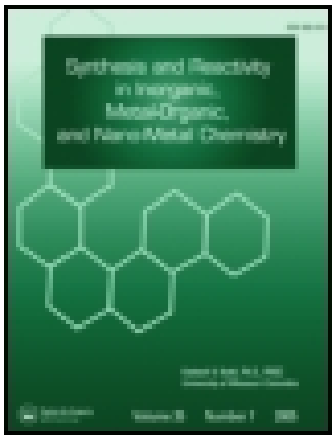

Synthesis and Reactivity in Inorganic, Metal-Organic, and Nano-Metal Chemistry

Publication details, including instructions for authors and subscription information:
http://www.tandfonline.com/loi/lsrt20

Synthesis, Molecular modeling and DNA binding of New Schiff base Ruthenium(II) complex and its Catalytic oxidation

Amira R.El-Shobaky[a]

[a] Department of Chemistry, Faculty of Science, University of Damietta, Damietta 34517, Egypt

Accepted author version posted online: 19 Feb 2015.

Synthesis, Molecular modeling and DNA binding of New Schiff base Ruthenium(II) complex and its Catalytic oxidation

Amira R.El-Shobaky*

Department of Chemistry, Faculty of Science, University of Damietta, Damietta 34517, Egypt.

*E-mail: aelshobaky@yahoo.com

Abstract

New Ruthenium(II) complex derived from 4-aminoantipyrine Schiff base (L). The structural feature has been confirmed through elemental, magnetic susceptibility and molar conductivity analysis. IR, UV-Vis and ^{1}H NMR spectral studies show that the complex has composition of [Ru LCl_2] type, suggesting an octahedral geometry around the central metal ion. DNA interaction studies throw spectroscopic and viscosity measurement confirmed that complex bind through intercalative mode, which confirmed by computational data throw the calculation of thermodynamic parameter. Also, catalytic oxidation of the Ru(II) complex was carried out showing that the complex is efficient catalyst for the oxidation .

Keywords: Ruthenium(II) complex; Catalytic Oxidation; DNA Studies ; Molecular modeling

1. Introduction.

Now days, Schiff bases of 4-aminoantipyrine and their complexes have a variety of applications in biological, clinical, analytical and pharmacological areas [1,2]. Basically, the mycological investigations and the fruitful results are facilitating the chemists to explore these compounds in the challenging pharmaceutical field [3–5]. A number of metal chelates are of current interest due to their important applications in nucleic acid chemistry as DNA probes of DNA structure in solutions, reagents for the mediation of strand scission of duplex DNA under physicochemical conditions [6-8**]**. The interaction between DNA and transition metal complexes is an important fundamental issue in life sciences [9]. This study is planned to isolate, characterize new Ru(II) complex derived from 4-aminoantipyrine Schiff base, studying the DNA binding mode and how it confirmed using the molecular modeling data , however, the ability of Ru(II) complex as catalyst in oxidation of organic compounds was studies.

2. Experimental.

2.1 Materials and general measurements**.**

All chemicals used are BDH (British Drug LTD, England) quality and used without further purification**.** The metal analysis determined by standard methods [10]. The elemental analyses (C and H) were determined by the standard micro methods in the microanalytical unit of Mansoura University, Egypt. Magnetic measurements were carried out at room temperature using Gouy's method, employing $Hg[Co(SCN)_4]$ for calibration purpose. IR spectra were recorded on a Mattson 5000 FTIR Spectrometer as KBr discs and UV-visible spectra were

measured in dimethylsulphoxide (DMSO) using an UV2-100 Unicam spectrophotometer. ^{1}H-NMR spectra were recorded on Prucker Ac 400 Spectrometer. Molar conductance measurements of the solid complexes (10^{-3} M) in DMSO at room temperature were measured using a type CD6NGT Tacussel Conductivity Bridge. Purity of the DNA was checked. All the solutions were adjusted with the Britton Robinson buffer (BR) solution (0.1 mol L^{-1}, pH 7.2), pH-metric measurements were made on a on a CG 808 (Schott Gerate, Germany) digital pH-meter with glass combination electrode, which was previously standardized with buffers of known pHs**.**

2.1. Syntheses of Schiff base (L).

According to the procedure previously described in the literature [11] an ethanolic solution (20 mL) of 4-aminoantipyrine (2.03 g, 0.01 mol) was added to an ethanolic solution of salicylaldehyde (1.06 g, 0.01 mol). On stirring the yellow colored solid (A) was separated. It was filtered and recrystallised from ethanol. The solid (A) (3.074 g, 0.01 mol) was added to an ethanolic solution (20 mL) of o-phenylenediamine (0.541 g, 0.005 mol). The mixture was refluxed for ca 30 h. The brown solid (L) product was separated. It was filtered and recrystallized from ethanol (Fig. 1). Yield: 74 %; m.p: 200 °C; Anal. calcd. for $C_{42}H_{38}N_8O_2$: C, 73.2; H, 5.5; N, 16.3; Found: C, 73.2; H, 5.4; N, 16.1.

2.2. Syntheses of Ruthenium (II) complex.

The Schiff base L (1 mmol) dissolved in hot ethanol (50mL) was added to a hot ethanolic solution (25 mL) of Ruthenium tri-chloride (1 mmol) and refluxed for 30 min. The resulting solution was reduced to one third on a water bath. The solid product with a green color separated

was filtered and washed with hot ethanol (Fig.2) Yield: 84 %; m.p: 300°C; Anal. calcd. for $RuC_{42}H_{38}Cl_2N_8O_2$: C, 57.7; H, 3.8 ; N, 13.3; O, 3.5; Ru, 11.2 ; Cl, 8.8 ; Found: C, 58.7; H, 4.5; N, 13.1; O, 3.7; Ru, 11.8; Cl, 8.3.

2.3. DNA binding studies:

The experiment involving the interaction of complex with double stranded fish sperm DNA has selected as the ds-DNA model because of its low cost, already availability, was conducted in Tris buffer pH 7.2 . The concentration of DNA in stock solution was determined by UV absorption at 260 nm using a molar absorption coefficient ε_{260} = 6600 L mol^{-1} cm^{-1}. Purity of the DNA was checked by monitoring the ratio of the absorbance at 260 nm to that at 280 nm. The solution gave a ratio of >1.8 at A_{260}/A_{280}, which indicates that DNA was sufficiently free from protein. The absorbance measurements were performed by keeping the concentration of the complex constant (1 x 10^{-4} M) while varying the DNA concentrations (1 x 10^{-4} M, 40, 60, …… and 160 µL). To quantitatively determine the binding strength of the complex, the intrinsic binding constant K_b of the complex with ds-DNA was obtained by monitoring the changes in absorbance of the complex with increasing DNA concentrations [12] .According to Eq. (1):

$$\mathbf{[DNA]/(\varepsilon_a - \varepsilon_f) = [DNA]/(\varepsilon_b - \varepsilon_f) + 1/(K(\varepsilon_b - \varepsilon_f)} \qquad \mathbf{(1)}$$

Where [DNA] is the concentration of DNA in base pairs, the apparent absorption coefficients ε_a, ε_f and ε_b are correspond to A_{obs}/[complex], the extinction coefficient for the free complex and extinction coefficient for the complex in fully bound form, respectively. The data were fitted of above equation with a slope equal to $1/(\varepsilon_a - \varepsilon_f)$ and y-intercept to $1/K_b$ $(\varepsilon_b - \varepsilon_f)$ and was obtained

from the ratio of the slope to the intercept [13]. The standard Gibbs free energy for DNA binding was calculated from the following relation [14] $\Delta G_b^o = - RT \ln K_b$ **(2)**

2.4. DNA binding analysis using viscosity measurements.

The viscosity experiments were conducted on Ubbelohole Viscometer, 10 ml of Tris buffer was transferred to the viscometer to obtain the reading of flow time, 10 ml of buffer solutions of 120 µM ds-DNA was taken in the Viscometer and a flow time reading was obtained that kept the DNA concentration constant, adding different concentration of the complex (40 – 160 µM) and the flow time was read as, the flow time of samples were measured after equilibrium was achieved. The buffer flow time was recorded as t^o. The relative viscosities for DNA in the presence (η) and absences (η^o) of the complex were calculated using the relation $\eta = (t-t^o)/t^o$, where t is the observed flow time in seconds. The values [15] of relative viscosity $(\eta/\eta_0)^{1/3}$ plotted against [Complex]/[DNA].

2.5. Computational details.

The theoretical calculations of the quantum chemistry were performed on a Pentium 4 (3 GHZ) computer using Hyper-Chem 8.0 program system. The molecular geometry of the ligand was optimized using molecular mechanics (MM^+) and molecular dynamics. The low lying obtained at PM3 using the Polak-Ribiere algorithm in RHF-SCF, set to terminate at an RMS gradient of 0.01Kcal $A^{o\,-1}mol^{-1}$ and convergence limit was fixed to $1x\ 10^{-8}$ Kcal mol^{-1} [16].

2.6. Catalytic Oxidation For the catalytic oxidation by [$Ru^{II}LCl_2$] complex, the organic substrate (1.0 mmol) was added to $NaIO_4$ (2.5mmol) in CCl_4-CH_3CN-H_2O (1:1:2; 20 ml) and the catalyst (0.02 mmol). The reaction mixture was stirred under reflex at 70^oC, then cooled and extracted with diethyl ether (3x20 ml). The ethereal layer was then dried with anhydrous Na_2SO_4 and the aldehyde or ketone content quantified as its 2,4-dinitrophenylhydrazone derivatives. The aqueous layer was acidified with 5M H_2SO_4 to PH2, extracted with diethylether (3x20 ml), dried and evaporated to give the acid [17].

3. Results and discussion

This complex is stable at room temperature and soluble in DMF and DMSO on the basis of analytical data the metal chelates are found to have 1:1 Metal ligand stichiometry. The molar conductivities (Λ_m) in DMSO at 25 ^oC is 17 ohm^{-1} cm^2 mol^{-1} .The analytical data indicates which are correspond to empirical formula that ligand is behaving as tetradentate in chelation.

3.1. Infrared spectra

The IR spectra provide valuable information regarding the nature of the functional group attached to the metal ion. The IR spectrum of the ligand shows a broad band in the region 3400-3600 cm^{-1}, assignable to intermolecular hydrogen bonded –OH groups. The appearance of this peak in the complex spectrum indicate that the –OH group is free from complexation. The spectrum of the ligand shows two different –C=N bands in the region 1652-1592 cm^{-1}, which are shifted to lower frequencies in the spectrum of the complex (1608 -1560cm^{-1}) indicating the involvement of –C=N nitrogen in coordination to the metal ion. The stretching wave number

due to N-N in the free ligand at 1045 cm^{-1} which slightly affected in the coordinated compound indicating that the unsharing. Accordingly, the ligand acts as a tetradentate chelating agent [18, 19] , bonded to the metal ion *via* the four nitrogen (–C=N) atoms of the Schiff base. Assignment of the proposed coordination sites is further supported by the appearance of medium bands at 507-455 cm^{-1} which could be attributed to ν (Ru-N) [20].

3.2. ^{1}H NMR spectra

^{1}H-NMR spectrum of the free ligand shows signal at δ 13.2 ppm which disappear upon adding D_2O, is attributable to phenolic –OH group present in the salicylaldehyde [21]. The presence of this peak noted for the Ruthenium complex confirms the –OH proton free from complexation [22]. The complex show singlet at δ 9.7 ppm due to presence of azomethine group proton and this signal shift down field in complex which indicate that proton remain unchanged during coordination and this shifting of azomethine proton signal in the spectrum of the complex down field suggesting deshielding of azomethine group due to coordination. A multiplet signl is appear at δ12.33 ppm due to 10 aromatic proton in ligand spectrum and these protons signal remain unchanged in complex spectrum [23].

3.3. Magnetic and Electronic absorption spectrum

The electronic spectra in dimethylsulphoxide for Ru(II) complex show three bands near 413,330 and 314 nm which may arise from $^{1}A_g \rightarrow {}^{1}T_{1g}$, $^{1}A_{1g} \rightarrow {}^{1}T_{2g}$ and ligand (π-dπ) to metal transitions, respectively, this indicates a low-spin octa-hedral arrangement around the diamagnetic Ru(II) [24,25].

3.4. DNA binding studies

Titration with electronic absorption spectroscopy is universally employed and an effective method to investigate the binding mode of DNA with a metal complex [26, 27] . The spectra were recorded as a function of the addition of the buffer solutions of pre-treated ds DNA to the buffer solutions of the complexes. If the binding mode is intercalation, the orbital of intercalated ligand can couple with the orbital of the base pairs, reducing the π–π* transition energy and resulting in bathochromism. If the coupling orbital is partially filled by electrons, it results in decreasing the transition probabilities and resulting in hypochromism [28]. The extent of the hypochromism in the metal- to – ligand charge transfer (MLCT) band is commonly consistent with the strength of intercalative interaction [29] (Fig. 3). The electronic absorption spectra of Ru(II) complex in the absence and presence of ds-DNA at a constant concentration of (10^{-4} M) in Tris buffer show that three λ_{max} at 286 nm and 330-314 nm attributed to π–π* excitation and 413nm due to MLCT which are given in (Fig. 4). By adding of DNA, the absorption intensity of MLCT band gradually increased. Moreover, addition of increasing amounts of ds-DNA resulted in a decrease of absorbance for the investigated complex. Representative spectrum illustrating this hypochromicity and the presence of isosbestic points observed for the interaction of complex with ds-DNA .The investigated complex could bind to DNA via intercalative mode .The value of binding constant of the investigated complex with DNA are smaller than that of reported for typical classical interceptors (7.7×10^3 L mol $^{-1}$) [30]. Also, the standard Gibbs free energy ΔG_b^o = - 131.78 kJ mol $^{-1}$. The negative value of ΔG for the complexation process suggests the spontaneous nature [31].

3.5. Viscosity Studies.

Spectroscopic data are necessary, but not sufficient to support a binding mode. To further clarify the nature of the interaction between the complex and DNA. Hydrodynamic methods such as viscosity measurements, which are sensitive to length increase or decrease of DNA, are regarded as the most effective means of studying the binding mode of complexes [32]. The relative viscosity of DNA solution increases significantly as the amount of complex increases, The values of $(\eta/\eta_{\circ})^{1/3}$ were plotted against [complex]/[DNA]. With the increase in the amount of the complex, the relative viscosity of DNA increases, indicating that intercalative as in (Fig. 5) .this may be due to the insertion of aromatic ring in Schiff base ligand into the DNA base pairs, increase in separation of the base pairs at the intercalation site, consequently increasing in DNA molecular length. Moreover, the sequences of the observed increase in values of viscosity was correlated the binding affinity to DNA, the information obtained from this work could be helpful to understanding of mechanism of the interaction of small molecules with nucleic acids, and should be useful in the development of potential props of DNA structure and conformation [33,34].

3.6. Molecular modeling of Ru(II) complex .

The molecular modeling of the complex was presented in (Figure 6). The molecular modeling complex is shown in **Table 2**. Inspection of data, it is observed that:

(i) The [Ru L Cl_2]complex has higher dipole moment suggesting that the asymmetric units have been estimated with respect to the center of mass as the origin, however the formation

of hydrogen bond, although the values themselves are independent of the choice of origin as the asymmetric unit [35]. The plots of the highest occupied molecular orbital (HOMO) and the lowest unoccupied molecular orbital (LUMO) for both the neutral asymmetric units are shown in figure 7, where the charge-transfer between the molecular partners is clearly evident.

(ii) The shape of [Ru L Cl_2] complex is found octahedral geometry as it expected for Ru(II) complex confirmed the data of electronic spectra and magnetic moment.

(iii) The heat of formation is positive quantity $\Delta H = 1641$ kj/mol, which indicates the dissociation is accompanied by absorption of heat and the process is endothermic [36].

(iv) Throw the theoretical data, the binding of complex with ds-DNA can be summarizes using the value of ΔH for calculation ΔS from the following equation:

$\Delta G = \Delta H - T\Delta S = - RT \ln K_b$ as in (Table 2). According to the thermodynamic data, interpreted as follows, the mode of interaction between Ru(II) complex and ds-DNA that $\Delta H > 0$ and $\Delta S > 0$, hydrophobic forces that cause hydrophobic solutes (both complex and DNA) to aggregate to reduce solvent-solute interface energy [37]. The ΔS values for the complex are positive, confirming that the complex formation is entropically favorable.

(v) The electrostatic potential on the iso electron density surface (Figure 8) .The maps indicate the donor acceptor sites for hydrogen bonding present in the proton- transfer complex. It is interesting to note that in the Ligand carries most of the negative potential (red) whereas the surface over ruthenium ion is with positive values (green and blue) clearly implying proton transfer between these molecules.

3.7. Catalytic oxidation

The catalytic oxidation of lower valent ruthenium complex in presences of NMO or hydroquinone as co-oxidants towards the oxidations of primary and secondary alcohols has been investigated .it was found that primary and secondary were oxidized to the corresponding carbonyl compounds. We tested the reported ruthenium complex $[Ru^{II}LCl_2]$ for possible organic catalytic oxidations by taking 0.02 mmol of the catalyst in CCl_4-CH_3CN-H_2O (1:1:2) solution with $NaIO_4$ (2.5 mmol)as co-oxidation with 1.0 mmol of substrate (Figure 9), the reactions being carried out for 3h in the case of alcohols and 4h in case of aryl halides, all at 70^oC . Aldehydes and ketons were detected and quantified as 2,4-dinitrophenylhydrazone derivatives and acid isolated and weighed as such, as shown in **Table1** . Blank experiments were conducted under similar conditions, but in the absences of complex; in all cases very small amounts of oxidation products were found [38].

4. Conclusion

Ruthenium(II) complex of the composition [Ru L Cl_2] has been synthesized with asymmetric tetradendate ligand which characterized on the basis of elemental analysis and spectral (IR, UV-Vis and ^1H NMR)data. An octahedral structure has been tentatively proposed for the complex. The DNA binding of Ru(II) complex has been examined by absorption spectroscopy and viscosity measurements, showed that bind intercalatively via their extended, planar ligand and higher hydrophobicity . However, using the molecular modeling for Ru(II) complex and calculation of physico-chemical parameter in a new summarized tool to confirm the binding mode between the Ru(II)complex and DNA intercalative mode. Also, the Ru(II)

complex showed efficient catalytic property for oxidation of both primary ,secondary and aryl halides in presences of $NaIO_4$ as co-oxidant for good application for the Ru(II)complex[38] .

Acknowledgements

The auther express her sincere thanks to the Damietta university faculty of sciences, chemistry department, central lab, for helping her for carrying out her research encourage and support .

References

[1] Hitoshi T.; Tamao N.; Hideyuki A.; Manabu F.; Takayuki M.; Polyhedron . 16 1997, 3787-3797

[2] Punniyamurthy T.; Kalra S. J. S.; Iqbal J.; Tetrahedron Lett. 1995,36, 8497 – 8712.

[3] Guoa W.; Escuer A.; Tanga M.; Jianga C. H.;Du M. ; Inorg. Chimica Acta. 2013 403, 142–146

[4] Raman N.; Sobhaa S.; Thamaraichelvanb A.; Spectrochim Acta . 2011 78(2) 888-898

[5] Raman N.; Raja J .D.; Sakthivel A .; J. Chem. Sci., 2007, 119, 4303–4310.

[6] Chan S.; Wong W.T.; Coord. Chem. Rev. 1995 .138.219–296.

[7] Pratviel G.; Bernadou J.; Meunier B.; Adv. Inorg. Chem. 1998. 45. 251–312.

[8] Radi A.; Khafagy A.; El-shobaky R.A.; El-mezayen H.; Journal of Pharmaceutical Analysis. 2013,3(2) 132–136.

[9] Liang F.; Wang P.; Zhou X.; Li T, Li Z.Y.; Lin H.K.; Gao D.Z.; Zheng C.Y; Wu C.T.; Bioorg. Med. Chem. Lett. 2004, 14, 1901–1917.

[10] A. I. A, Vogel, Text Book of Quantitative Inorganic Analysis, 3rded. ; Longman London, 1975.

[11] Raman N.; Thalamuthu S.; Raja J.D.; Neelakandan M. A. ; Banerjee S.; J. Chil. Chem. Soc., 2008, 53 (1) 1424-1428.

[12] Abdel-Rahman L.H.; El-Khatib R.M.; Nassr L.A. E.; Abu-Dief A.M.; journal of Molecular structure . 2013,1040, 9-18.

[13] Sabolova D.; Kozurkova M.; Plichta T.; Ondrusova Z.; Hudecova D.; Simkovic M.; Paulikova H.; Valent A.; Int.J. Biol. Macromol. 2011 ,48, 319-325.

(14) Sangeetha K.; Gowda R; Bhojy N.; Vinay H.S.; . Kumar B; Sudhamani C.N; Sudeep H.V.; Naik Ravikumar T.R.; Krishnamurthy G. ; Spectrochimica Acta Part. 2013, 105. 229–237.

[15] Kelly T. M.; Tossi A. B.; McConnell D. J.; Strekas T. C.; Nucleic Acids Res. 1985, 13, 6017-6034.

[16] El-Ayaan U.A.; Abdel-Aziz A. M.; Al-Shihry S.; European Journal of Medicinal Chemistry.2007, 2, 1-9.

[17] Balasubramanium K.P.; Karvembu R.; Prabhakran R.;; Chinnusamy V.; Natarajan K.; Spectrochemica.Acta, 2006, 65, 678-683.

[18] Sigman D.S.; Graham D.R.; Aaurora V.D.; J. Biochem. 1979, 254, 1264-1269

[19] Ramana N.; Selvana A.; Manisankarb P. ; Spectrochim Acta .2010,76(2) 161-173.

[20] Nakamoto K., Infrared Spectra of Inorganic and Coordination Compound. Wiley , New York (1986).

[21] Zifiropoulous T.F.; Plakatous J.C. ; Pertepes S.; Polyhedron. 1991,10, 2405-2521.

[22] Bekheit M .M; Gad Allah M. T.; El-Shobaky .R A.; (2013), http://dx.doi.org/10.1016/j.arabjc.2013.07.025

[23**]** Silver Stein R.M., Webster F.X., Spectrometric Identification of Organic Comp. Wiley, New Delhi India, (2007).

[24**]** Kelly J.M.; Tossi A.B.; . Mc D.J; Connell, Uigin C.O.; NuL. Acidsv Res, 1985 13,6017-6034.

[25]El-Shahawi M.S.; Shoair A.F. ; Spectrochim Acta.2004, 60, 121-127.

[26] Liu X. W.; . H. Li; Zheng K.C; H.Chao; Ji L.N.; J. Inorg. Bio.Chem. Soc. 2005, 99,2372-2380.

[27] Thomas R.; Pal S.; Datta A.; Marchewka M.; Ratajczak H.; Pati S.; Karni. G., J. Chem. Sci., 2008, 120, 6613–620.

[28] Abdel-Rahman L.H.; El-Khatib R.M.; E.Nassr L.A.; Abu-Dief A.M.; Spectrochemica acta . 2013,111, 226-276.

[29] Chao H.;Mei W.J.; Huang Q. W.; Ji L. N.; J. Inorg. Bio.chem, 2002, 92, 165-170.

[30] liu Y.; Mei W.; Lu J.; Zhao H.; He L.; Wu F.; J. Coord. Chem. 2008, 61, 3213-3224.

[31] Btahim A.A.; Adel A.M.; Abd El-wahab Z.A.; Al-Shemy M.T.; Carbonhdr. Polym .2011, 83, 89 - 94.

[32]Suah M. P.; Shim B. Y. ; Yoon T. S; Inorg. Chem. 1994, 33, 5509-5514.

[33] Liu C. L.; Zhou J. Y.; Li Q. X.; Wang L. J.; . Liao Z. R.; Xu H. B.; J. Inorg. Biochem. 1999, 75233- 240.

[34] Feng Q.; Li V.Q.; Jiang Y.Y.; Analytica Chimica Acta. 1997 ,344(3),79-104.

[35] Users manual; XD program version 4. 2003;10.

[36] Atkin P. W.; Physical chemistry (Oxford University)(2002)7th edn.

[37] Shahabadi N.; Ghasemian Z; Hadidi S.; Bio.Inorg.Chemistry and Application ,vol 2012,doi:10.1155/2012/126451

[38] Anitha P.; Manikandan R.; Endo A.; Hashimoto T.; Viswanathamurthi P.; Spectrochim Acta . 2012, 99, 174-180.

Table 1. Catalytic Oxidations by [Ru L Cl_2] (L= Schiff base derived from 4-aminoantipyrine salicylaldehyde and o-phenylenediamine) complexes[a)]

Substrate	[Ru LCl_2]	
	Yield %	**Turn Over**
Benzyl alcohol	**58%[ald], 15%[ac]**	**42**
3,4-Dimethoxybenzyl alcohol	**68%[ald], 13%[ac]**	**41**
α-Tetralol		**46**
Benzohedrol	**88%[k]**	**30**
Benzylchloride	**74%[k]**	
p-methoxybenzylchloride		**33**
	48 %[ald], 18%[ac]	**52**
	85%[ald], 20%[ac]	

[a] Oxidation of alcohols were carried out for 3h, those of aryl halaides for 4h, all at 70^0C by using 0.02 mmol of catalyst, 2.5 mmol of $NaIO_4$ (co-oxidant) in CCl_4 –CH_3CN-H_2O(1:1:2, 20 cm^3), [ald] corresponding aldehyde, [ac] corresponding acid, [k] corresponding ketone. Turnover = moles of product/moles of catalyst;the product determined by Gc and complared with analyses of authentic samples.

Table 2. Parameters of the molecular modeling of [Ru L Cl_2] **complex.**

Patameters	Total energy **(kcal/mol)**	Binding energy **(kcal/mol)**	ΔH **(kcal/mol)**	Electronic Energy **(kcal/mol)**	Dipole Moment **(Debyes)**	ΔH **(kJ/mol)**	ΔS **(KJ/mol/K)**	HOMO **(eV)**	LUMO **(eV)**
[Ru^{II} L Cl_2] at 298^oK using MM^+	**-200595**	**-10002**	**392.135**	**-2566367**	**12.1**	**1641**	**5. 948**	**-7.170098**	**-1.3428**
Ru^{II} L Cl_2] at 304.76^o K Molecular	**-9837.08**	**-9921.56**	**472.29**	**-2570850**	**12.6**	**1976**	**35.296**	**-7.143376**	**-1.2859**

dynamics									

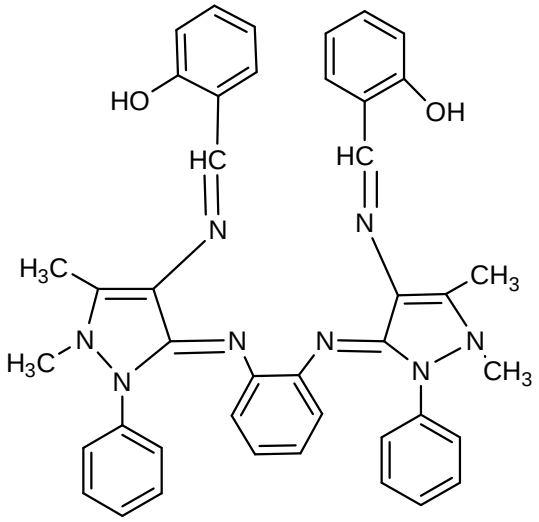

Figure 1. Structure of Schiff base ligand L

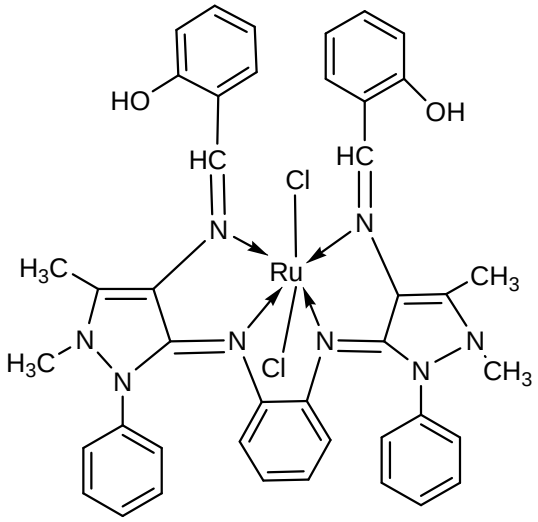

Figure 2 . Structure of Ruthenium(II) complex

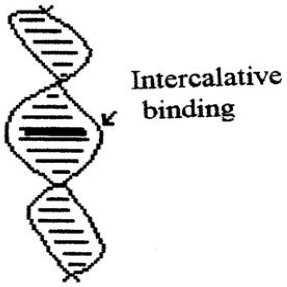

Figure 3. Intercalation mode of complex with DNA

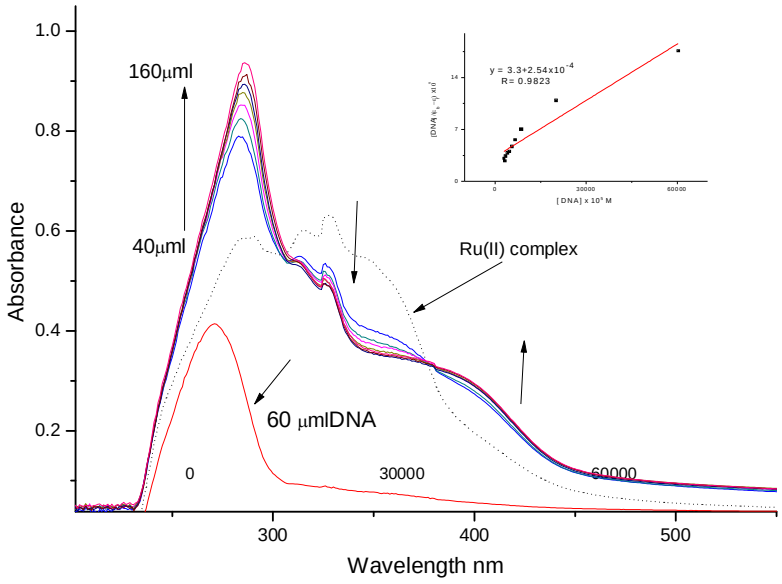

Figure 4. Electronic absorption titration curve of Ru(II) complex in the absences and presence of increasing amount of DNA: 40 -160 μM in 5 mM Tris-HCl buffer (pH 7.2). [Ru(II) complex = 150 μM. With incubation period of 30 min at 37°C. Inset Plot of [DNA]/ (ε_a- ε_f) versus [DNA].

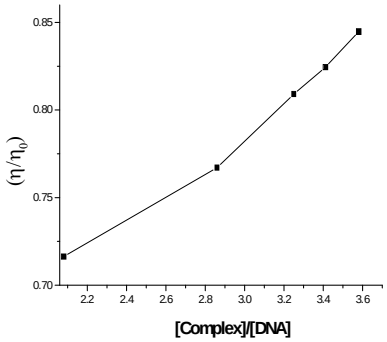

Figure 5. The effect of relative viscosity of DNA under the influence of increasing amount of Ru(II) complex in Tris-HCl buffer (pH 7.2).

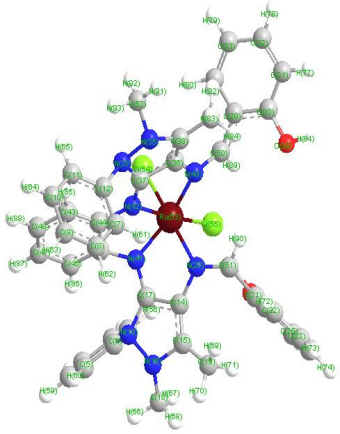

Figure 6 . Molecular modeling of [Ru L Cl_2] using Hyper-Chem 8.0 program optimized using molecular mechanics (MM^+) at PM3 using Polak-Ribiere algorithm.

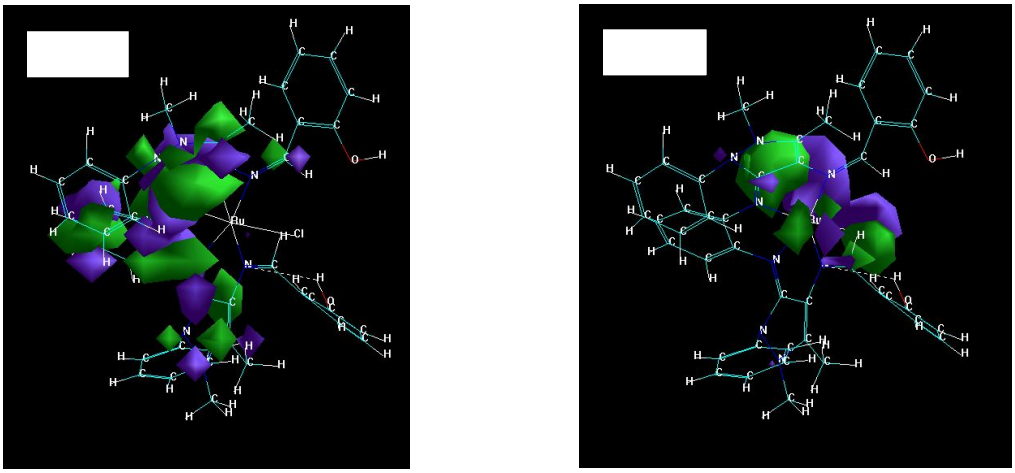

Figure 7. Frontier orbitals for Ru(II) complex

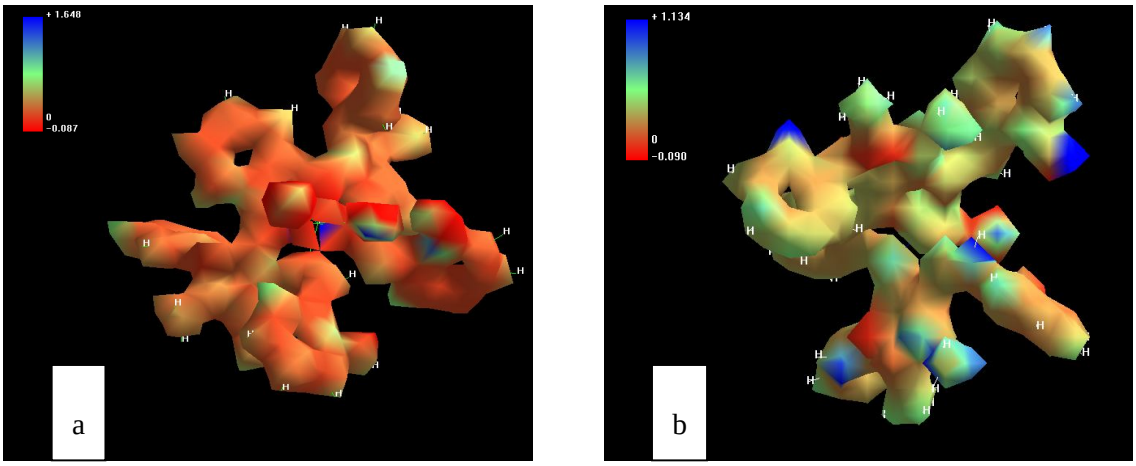

Figure 8. Electrostatic potential for Ru(II) complex , iso-density surface; a color gradient is applied to show the change from electronegative (towards red) to electropositive (towards blue) regions using (a) MM+, (b) Molecular dynamics at PM3.

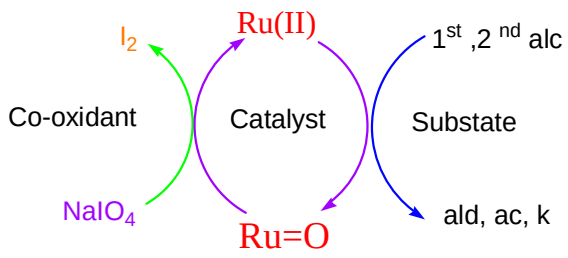

Figure 9. Catalytic cycle for primary alcohols to aldehydes and acids, secondary alcohols to ketones and aryl halaides to aldehydes and acids in presences of $NaIO_4$ as co-oxidant.

